One step synthesis of 3D $BaTiO_3$@C for novel electromagnetic shielding of epoxy composites

Dongmei Zhang[1], Yongzhi Yang[2], Xiaoqian Liu[2], Runhan Xu[2], Yuchao Li[2,*], Wenbin Guo[1], Shuangshuang Wang[2], Qian Xie[2], Chengzhu Liao[3,*]

[1]School of Mathematical Sciences, Liaocheng University, Liaocheng 252059, China
[2]School of Materials Science and Engineering, Liaocheng University, Liaocheng 252059, China
[3]Department of Materials Science, South University of Science and Technology, 518055, China

Abstract: The ever-increasing electromagnetic interference (EMI) pollution becomes an important issue in current environmental protection and human society. In this work, 3D $BaTiO_3$(3DBT)@C porous ceramic framework was one-step fabricated by sol-gel method using environmentally friendly cleanroom wipers as template and calcined under inert atmosphere. Subsequently, epoxy (EP) resin was reversely incorporated into the above 3DBT@C network, resulting in the 3DBT@C/EP composite. Results showed that the cleanroom wiper was calcined and transformed into amorphous carbon within the 3DBT, leading to the excellent electrical conductivity of 3DBT@C. The reverse infiltration of EP maintained the successive 3DBT framework and excellent conductivity, thus endowing the 3DBT@C/EP composite with a good electromagnetic interference shielding effectiveness (EMI SE) as high as 36.6 $dB \cdot mm^{-1}$ at 10.2 GHz. The absorption mechanism of EMI prevailed the EMI SE due to the large Ohmic loss and porous 3D network, implying potential applications in flexile shielding materials.

1. Introduction

The wide application of electronic devices has caused serious problems of electromagnetic interference (EMI) pollution, which seriously destroys the stability of equipment and does harm to human health. Therefore, much effort has been made in the scientific community and industry to the development of new and highly efficient EMI materials. Most metals or alloys are naturally good EMI materials; however, it suffers from poor flexibility and processability. In this regard, conductive polymer composites (CPCs) have gained more and more attention in the past decades, due to the obvious advantages over traditional metal-based EMI shielding materials, including lightweight, good flexibility, corrosion resistance, easy processing and high EMI shielding effectiveness (EMI SE). Previous studies have shown that the inclusion of conductive nanofillers, such as graphene, carbon nanotubes (CNTs), carbon black (CB) and MXene in CPCs, can achieve high EMI SE values near the percolation threshold. However, they usually have narrow bandwidth, poor absorption, and bad impedance-matching [1,2]. Recently, incorporating conductive nanofillers into three-dimensional (3D) interconnected networks to form aerogels and foams has been proved to be a successful strategy for decreasing the percolation threshold and increasing EMI performance of CPCs [3,4]. He et al. reported an enhanced EMI performance of epoxy composites with hierarchical MXene/graphene aerogel structure [5]. The EMI SE achieved as high as 68 dB with the deposition of MXene into graphene aerogels. The large EMI SE not only depends on the excellent electrical conductivity of Mxene/graphene, but also ascribes to the hierarchical design of the porous structure. Various studies have shown that the design of porous structure is a good choice in the exploration of high-performance EMI SE of CPCs. The specific surface area of the material is substantially increased, which in turn scatters and multiple reflects EM waves in the aperture, enhances the interaction with absorbers. [6,7] Additionally, the dielectric constant and dielectric loss can be adjusted by changing the content of carbon materials, thus optimizing the impedance matching [8,9].

In this work, a novel epoxy (EP) based EMI composite material was facilely obtained by reversely infiltrating EP resin into a porous conductive 3DBT@C ceramic network, which was easily one-step constructed by sol-gel method using environmentally friendly cleanroom wipers as template. The sol-gel method have the advantanges over other methods in the relatively mild reactive conditions and environmental friendliness. In addition, the low-cost cleanroom wiper possessed interwoven porous structure, which can be used as template to construct porous carbonaceous materials for catalysis and supercapacitor purposes. Furthermore, it contained 55% cellulose and 45% polyester fiber, which can be easily decomposed naturally to some extent. The synthesized BT@C possessed a successive 3D network structure with excellent electrical conductivity due to the presence of amorphous carbon,

* Corresponding author: Yuchao Li, liyuchao@lcu.edu.cn; Chengzhu Liao, liaocz@sustech.edu.cn

thus endowing the 3DBT@C/EP composite with excellent EMI SE. It is believed that the absorption mechanism of EMI caused by the Ohmic loss and the porous 3D BT@C network structure prevails the EMI SE, providing a facile strategy of obtaining high efficiency EMI materials.

2. Experimental

2.1 Materials

Barium acetate ($C_4H_6BaO_4$, >99%), tetrabutyl titanate ($C_{16}H_{36}O_4Ti$, >99%), and acetylacetone ($C_5H_8O_2$, >99%) were supplied from Tianjin Kemiou Chemical Reagent Co., Ltd. Glacial acetic acid ($C_2H_4O_2$, >99%) was acquired from Shanghai Aladdin Biochemical Technology Co., Ltd. Ethylene glycol monomethyl ether ($C_3H_8O_2$, >99%) was obtained from Sigma-Aldrich. Cleanroom wipers was purchased from Kunshan cleanroom wipers Factory in Jiangsu Province, China. Poly(sodium 4-styrenesulfonate) (PSS, M_W=1,000,000) was purchased from Sigma-Aldrich. Epoxy (EP, E51, eq/mg: 0.5) was purchased from Wuhuigang Adhesive Co., Ltd.

2.2 Preparation of 3DBT@C network and 3DBT@C/EP composite

The synthesis procedure of 3DBT@C and 3DBT@C/EP composite is shown in Fig. 1. Porous 3DBT@C ceramic network was one-step prepared by sol-gel method using cleanroom wipers as template. Firstly, 6.38g $C_4H_6BaO_4$ was dissolved in 20 ml $C_2H_4O_2$ at 80°C, and then appropriate amount of $C_{16}H_{36}O_4Ti$ (8.8 ml) (Ba^{2+}:Ti^{4+}=1:1), ethylene glycol monomethyl ether (26 ml) were added to the above barium sources with continuous stirring at room temperature. In the meanwhile, a small amount of acetylacetone (0.05 ml) was added to obtain the BT precursor solution. The interwoven 3D skeleton of cleanroom wiper (40×40×0.1 mm^3) was then immersed into the precursor for 2 hours with the aid of ultrasonication (Step I in Fig. 1). The BT sol was infiltrated into the above interwoven cleanroom wiper. The template with fully absorbed BT sol was then placed in a 60 ºC oven for 24 hours to remove the $C_5H_8O_2$ and obtain the BT gel (Step II in Fig. 1). Finally, the cleanroom wipers template containing BT gel was calcined in a tube furnace at 1100 ºC for 3 hours under Argon (Ar) atmosphere. Due to the protection of inert Ar gas, the cleanroom wiper was not thorougly decomposed into gases, but carbonized into amorphous carbon as verified form the XRD patterns of Fig. 2(a). Interestingly, a porous 3D framework of BT@C was obtained (Step III in Fig. 1) based on the 3D skeleton of cleanroom wiper. For comparison, the BT gel was calcined at 1100 ºC under air atmosphere, obtaining the 3DBT network because the cleanroom wiper was burned out during calcination. The fabrication of 3DBT@C/EP and 3DBT/EP composites were conducted by reversely introducing the EP resin into the obtained 3DBT@C and 3DBT network with the aid of suction filtration to obtain a saturated composite (Step IV in Fig. 1).

2.3 Characterization

The internal 3D structure and morphology of the 3DBT@C ceramic and 3DBT@C/EP composite were observed by X-ray diffraction spectrometer (XRD, Bruker, D8-Advance) in 2θ range form 10 to 80° and field emission scanning electron microscopy FESEM (Carl Zeiss, SIGMA500). The thermal analysis was characterized by a simultaneous thermal analyzer (STA 449C, Netzsch) with a temperature rise from 20 to 800°C and a heating rate of 10 ºC·min^{-1}. The EMI SE of the composites was characterized in a transmission-reflection mode by a vector network analyzer (Agilent N5247A) in the frequency range from 8.2 to 12.4 GHz. The total EMI SE (SE_T), absorption SE (SE_A), reflection SE (SE_R) have the relationship as [10,11]:

$$SE_T = -10\,log\,T \quad (1)$$

$$SE_R = -10\,log(1-R) \quad (2)$$

$$SE_A = SE_T - SE_R = -10\,log(T/(1-R) \quad (3)$$

where T, R, and A are the transmission, reflection, and absorption coefficients, respectively, have $T+R+A=1$.

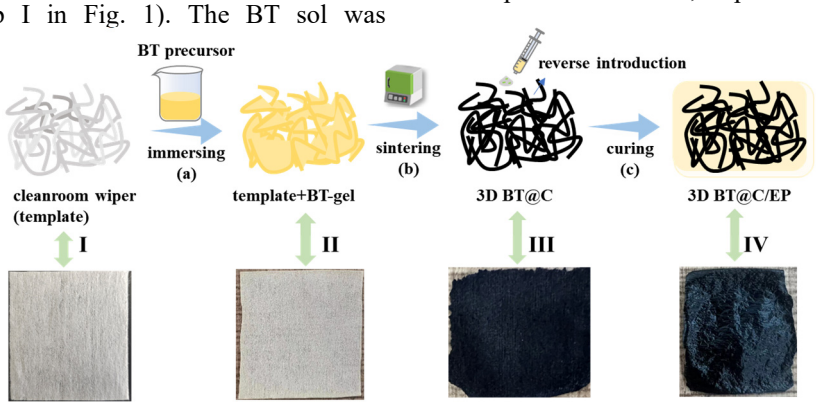

Fig. 1 Process of the preparation of 3DBT@C/EP composite

3. Results and Discussions

Fig. 2(a) illustrates the XRD patterns of the calcined 3DBT@C, 3DBT and cleanroom wiper. It is seen from Fig. 2(a) that the calcined cleanroom wiper has no distinct characteristic peaks, indicating amorphous carbon (C) structure during carbonation under high temperature. After calcination at 1100 ºC under Ar atmosphere, many distinct peaks located at 2θ=22.2º, 31.6º, 38.9º, 45.2º, 51.0º, 56.3º, and 65.8º correspond to the (100), (110),

(111), (002), (210), (211), and (220) diffractions of 3DBT@C, respectively. These characteristic peaks of 3DBT@C are the same to 3DBT calcined at 1100 °C under Air atmosphere, further indicating the amorphous carbon structure that has no big influence to the crystal of 3DBT. However, it is seen from the enlarged XRD curves around 45° that the 3DBT calcined under air atmosphere splits into two peaks (45° and 45.4 °), indicating the presence of a small amount of tetragonal phase BT, while the 3DBT@C is just the main cubic BT structure. In addition, the obtained 3DBT@C was further burned in TGA instrument under O_2 atmosphere. There is a weight loss in 3DBT@C due to the burning of amorphous carbon, implying that the concentration of C is about 14.2 wt%.

Fig. 3 shows the structure and morphology of the synthesized 3DBT@C and 3DBT ceramics. It is seen from Figs. 3(a) and 3(d) that the obtained 3DBT@C and 3DBT have similar interwoven skeleton to the pristine cleanroom wiper as reported in our previous work [12], which is porous and successive in three dimensions. What's more, the grain size of BT in 3DBT@C (Fig. 3(b) and 3(c)) is ambiguous due to the presence of amorphous carbon as compared with that of 3DBT (Fig. 3(e) and 3(f)). What's more, a needle-like product can be observed in the 3DBT@C (Fig. 3(c)) in comparison with 3DBT (Fig. 3(f)), which may be ascribed to the fibric carbon.

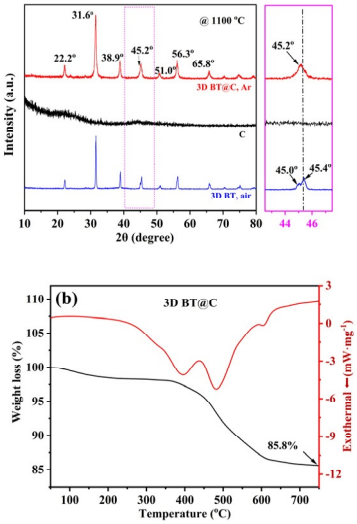

Fig.2 (a) XRD patterns and (b)TGA analysis of the synthesized 3DBT@C ceramic

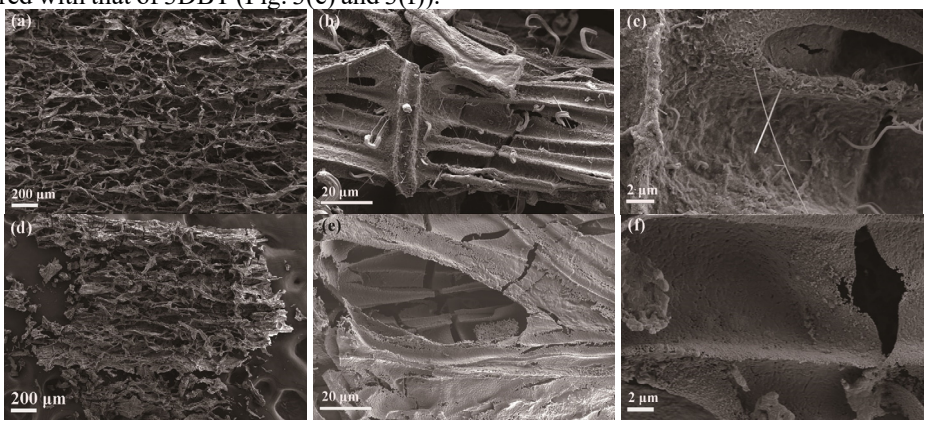

Fig. 3 Low and high magnification SEM images of (a)-(c) 3DBT@C, (d)-(f) 3DBT sintered at 1100 °C

Fig. 4 shows representative SEM images of 3DBT@C/EP composite. It is seen from Fig. 4(a) that EP was successfully infiltrated into the 3D network structure of 3DBT@C. Due to the large surface energy of 3DBT@C, the epoxy has good affinity with 3DBT@C (Fig. 4(b)). What's more, the 3D skeleton of 3DBT@C was not destroyed and still maintained a continuous network by the addition of EP, endowing the composites with good electrical conductivity comparable to that of the 3DBT@C ceramic, further indicating the successive 3D conductive network of composite. Fig. 4(c) further verifies the unchanged crystalline structure of 3DBT@C in the composites.

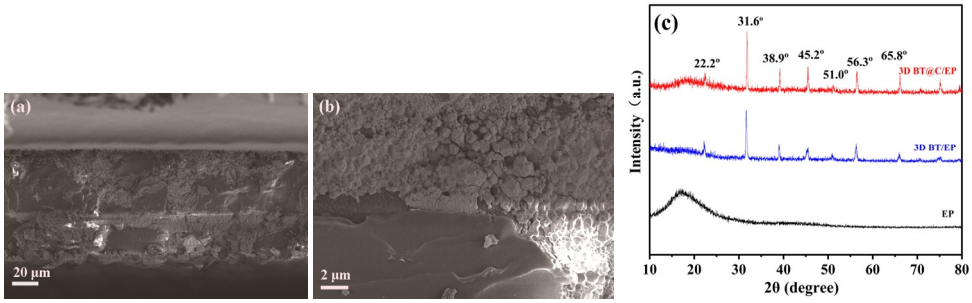

Fig. 4 (a) Low and (b) high magnification SEM images and (c) XRD spectra of 3DBT@C/EP composite

Fig. 5 displays the conductivity and EMI SE performance of 3DBT@C/EP composite. As illustrated in Fig. 5(a), the conductivity of the obtained 3DBT@C/EP composite calcined at 1100 °C possesses a high conductivity of 0.41 $S \cdot cm^{-1}$, a little higher than that of 3DBT@C ceramic calcined at 1000 °C, which may ascribe to the formation of large grain size of 3DBT@C and more successive conductive network. Figs. 5(b) and 5(c) illustrate EMI SE properties of 3DBT@C/EP composite. It is seen that the composite maintains a high EMI SE of 36.6 dB in the tested frequency range, implying excellent electromagnetic properties. It is known that the EMI SE of a material originates from the reflection and absorption principles. The SE_R is due to the

impedance mismatch between air and absorber, while the SE_A results from the ohmic loss, the polarization loss and the magnetic loss [13]. It is seen form Fig. 5(c) that the SE_R of 3DBT@C/EP composite is very small, indicating that the 3DBT@C structure absorbs most WM waves. The contribution of SE_A is more than 97.8% to the total EMI SE. From the literature, SE_R and SE_A can be calculated as [14]:

$$SE_R = 10\,log[\,\sigma_{ac}/16\omega\varepsilon_0\mu_r] \quad (4)$$

$$SE_A = 20t\sqrt{\omega\sigma_{ac}\mu_r/2} \quad (5)$$

where σ_{ac} is the AC conductivity, ω is the angular frequency, ε_0, μ_r, δ and t are the free space permittivity, relative magnetic permeability, skin depth and thickness of the shielding material, respectively. Therefore, it can be concluded that the Ohmic loss is the main reason for the large absorption. In addition, the special porous and hollow structure of 3DBT@C greatly reduces the material density and provides new channels for EM transmission, which further leads to the excellent wave absorption to the CPC. In addition, the facile construction of 3D ceramic network and the advantages of light and flexibility provide a good prospect for the application of EMI materials.

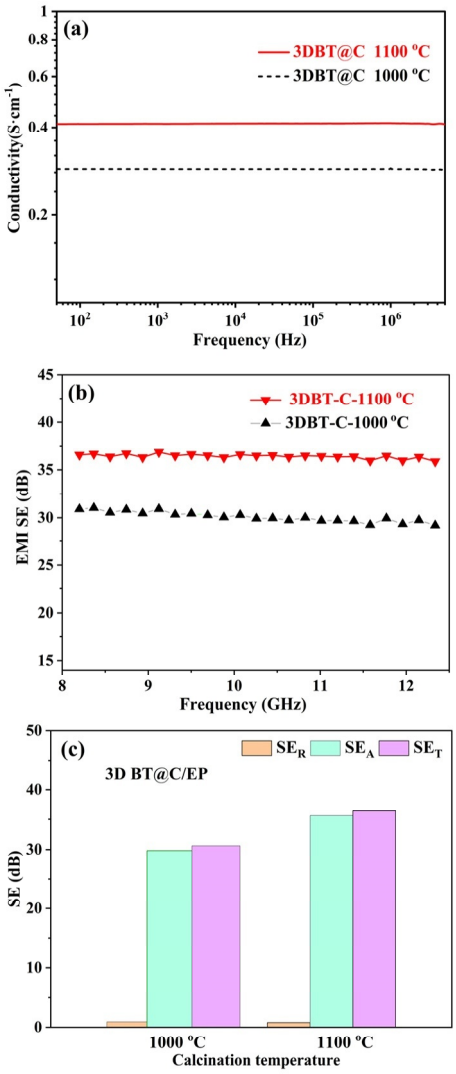

Fig. 5 (a) conductivity, (b) EMI SE and (c) SE_A and SE_R of 3DBT@C/EP composite

4. Conclusions

A 3DBT@C porous ceramic network was one-step synthesized by sol-gel method using cleanroom wipers as template and calcined under Ar atmosphere. The 3D interwoven structure of cleanroom wiper determined the final structure of porous 3DBT@C, therefore, a proper density and filament winding of cleanroom wiper is necessary to form a successive 3DBT@C. XRD patterns verified the presence of amorphous carbon, which led to the excellent electrical conductivity of 3DBT@C network. The large surface area enabled the infiltration of epoxy (EP) resin, resulting in a dense 3DBT@C/EP composite film with successive 3DBT@C framework and excellent conductivity, thus endowing the composite with excellent EMI SE as high as 36.6 dB·mm^{-1}, demonstrating potential applications in EMI materials.

Acknowledgments

We appreciate very much the financial support from NSFC of China (No. 52177020); NSFC of Shandong Province (ZR2021MB056); Student Innovation and Entrepreneurship Project of Liaocheng University (CXCY2022184 & CXCY2023015).

References

1. Z.Y. Guo, W.T. Zhang, E.J. Ding, X. Li, Compos. Part A 177, 107940 (2024)
2. Z.M. Jiang, S.J. Li, T. Park, Y. Kim, et al. J. Alloys Compou. 987, 174256 (2024)
3. Dandapani, K. Devendra, Revannasiddappa, K.R. Vishnu, Mater. Today: Proceed. 66, 1664 (2022)
4. C.L. Dong, S.J. Wang, P. Zhang, D.Y. Lei, B.B. Yin, et al. Mater. Today Phys. 42, 101373 (2024)
5. W.R. Zhang, J. Zhang, J.L. Xie, F.F. Su, Y.C. Li, D.D. Yao, et al. Compos. B: Eng. 274, 111230 (2024)
6. K. Li, Y. Fu, X. Yin, Y. Jiao, Q. Song, Compo. Sci. Technol. 222, 109407 (2022)
7. X. Ye, Z. Chen, S. Ai, B. Hou, J. Zhang, et al. J. Adv. Ceram. 8, 479 (2019)
8. D. Fan, B. Wei, R. Wu, J. Zhou, C. Zhou, Mater. Sci. 56, 6830 (2021)
9. L. Long, J.Q. Yu, Y.Q. Li, Y. Li, W. Zhou, Compos. Sci. Technol. 250, 110531 (2024)
10. U. Hwang, J. Kim, M. Seol, B. Lee, I.K. Park, J. Suhr et al. ACS omega 7, 4135 (2022)
11. J. Wang, R. Wu, J. Feng, J. Zhang, L. Hou, M. Liu. Trans. Nonferrous Met. Soc. China 32, 1385 (2022)
12. X. Bi, W. Xue, Y. Yang, Z. Wang, Z. Wang, Y. Li et al. Compos. Commun. 40, 101575 (2023)
13. X. Li, T. Xu, W. Cao, M. Wang, F. Chen, et al. Chem. Eng. J. 464, p. 142595. (2023)
14. W.T. Yu, J.H. Lin, Z.Z. Zhao, J.Y. Fang, Z.Q. Wang, et al. RSC Adv. 14, 9716 (2024)